

This paper is published as part of a *CrystEngComm* themed issue entitled:

## New Talent

*Showcasing the strength of research being carried out by tomorrow's leaders in the field of crystal engineering in its broadest sense, including crystal growth*

Guest Editor and Chair of the *CrystEngComm* Editorial Board:  
Professor Neil Champness  
University of Nottingham, UK

Published in [issue 8, 2010](#) of *CrystEngComm*

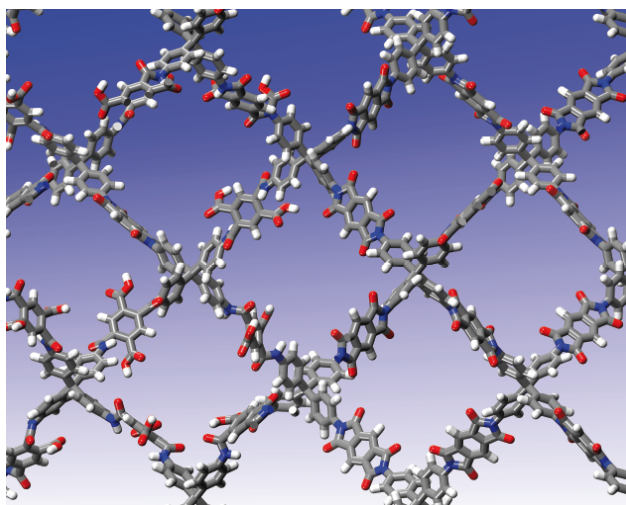


*Image reproduced with permission from Abbie Trewin*

Other articles published in this issue include:

[Dipyrrin based homo- and hetero-metallic infinite architectures](#)

Stéphane A. Baudron, *CrystEngComm*, 2010, DOI: 10.1039/c001020k

[Self-assembly of 1,4-cis-polybutadiene and an aromatic host to fabricate nanostructured crystals by  \$\pi\$ ...CH interactions](#)

Silvia Bracco, Angiolina Comotti, Patrizia Valsesia, Mario Beretta and Piero Sozzani  
*CrystEngComm*, 2010, DOI: 10.1039/c002931a

[Searching for novel crystal forms by \*in situ\* high-pressure crystallisation: the example of gabapentin heptahydrate](#)

Francesca P. A. Fabbiani, Demetrius C. Levendis, Gernot Buth, Werner F. Kuhs, Norman Shankland and Heidrun Sowa, *CrystEngComm*, 2010, DOI: 10.1039/b924573a

[Postsynthetic diazeniumdiolate formation and NO release from MOFs](#)

Joseph G. Nguyen, Kristine K. Tanabe and Seth M. Cohen  
*CrystEngComm*, 2010, DOI: 10.1039/c000154f

Visit the *CrystEngComm* website for more cutting-edge crystal engineering research  
[www.rsc.org/crystengcomm](http://www.rsc.org/crystengcomm)

# Control over the nucleation process determines the framework topology of porous coordination polymers†

Mio Kondo,<sup>a</sup> Yohei Takashima,<sup>b</sup> Joobeom Seo,<sup>c</sup> Susumu Kitagawa<sup>\*abc</sup> and Shuhei Furukawa<sup>\*ac</sup>

Received 10th March 2010, Accepted 22nd June 2010

DOI: 10.1039/c004066e

In this contribution, we present a method to selectively synthesize crystal polymorphs of  $[\text{Zn}_2(\text{bdc})_2(\text{dabco})]_n$  (**1**) and  $[\text{Zn}_2(\text{bdc})_2(\text{bpy})]_n$  (**2**), either the pillared 2D square-grid nets ( $1_{sq}$  or  $2_{sq}$ ) or the pillared 2D Kagomé nets ( $1_{kgm}$  or  $2_{kgm}$ ) by simply changing the crystallization temperature.

Porous coordination polymers (PCPs) or metal–organic frameworks (MOFs),<sup>1</sup> constructed by the self-assembly of metal ions and organic linkers, have attracted much attention because of their characteristic porous properties in industrial applications such as selected gas adsorption,<sup>2</sup> heterogeneous catalysts,<sup>3</sup> and chemical sensing.<sup>4</sup> One of the great advantages of PCPs is that we can easily tune the size and properties of the pores by functionalizing organic linkers or by changing the framework topology. There have been, indeed, numerous studies to control their properties using these methods.<sup>1–4</sup> However, the control of the connectivity between metal clusters still mostly relies on the fruit of serendipity.<sup>5</sup>

The nucleation process is the most important step to determine the crystal phase of the system, since the alteration of the conditions often leads to several different crystal structures for the same initial chemical system, so-called polymorphism.<sup>6</sup> Therefore, an understanding of the nucleation process of PCPs provides a considerable insight into the synthetic procedure of PCP materials as they are obtained as crystalline materials. In this contribution, we aimed to establish a methodology to systematically control the connectivity between metal clusters in PCPs by controlling the nucleation process. We chose the zinc paddle-wheel cluster with benzenedicarboxylate (bdc) and diazabicyclo[2,2,2]octane (dabco),  $[\text{Zn}_2(\text{bdc})_2(\text{dabco})]_n$  (**1**) as our object. Our method could be transposed successfully to a system using a longer pillar, giving the new  $[\text{Zn}_2(\text{bdc})_2(\text{bpy})]_n$  (**2**, bpy = 4,4'-bipyridine).

Two polymorphs of  $[\text{Zn}_2(\text{bdc})_2(\text{dabco})]_n$  have been reported so far; one is a tetragonal framework ( $1_{sq}$ , Fig. 1(a)),<sup>7</sup> in which 2D square-grid sheets constructed by Zn paddle-wheel units and bdc are connected by dabco pillar ligands, the other is a trigonal framework ( $1_{kgm}$ , Fig. 1(b))<sup>8</sup> with 2D Kagomé nets instead as layers (*sql* indicates

the square-grid motif and *kgm* the Kagomé motif).<sup>‡</sup> The previous reports demonstrated the selective syntheses of  $1_{sq}$  and  $1_{kgm}$  by the templating effect of solvents in solvothermal reactions,<sup>8a</sup> or that of anions for mechanochemical synthesis.<sup>8b</sup> Although the templating agent is efficient enough to decide on the polymorphism, the origin of the effect is unclear. In this contribution, we aimed to control the polymorphism without changing the solvent system<sup>§</sup> in order to identify the key factors for a selective synthesis; thereby establishing a systematic route to synthesize PCPs with a desired topology.

It is reasonable to assume that the crystallization process of PCPs from solution occurs first with the generation of soluble oligomers *via* the coordination interactions,<sup>9</sup> followed by the increase in size and concentration of oligomers leading the system to super-saturation. Once the nucleation has been initiated from this super-saturated solution, and crystals can grow. Furthermore, if the reaction temperature is high enough to dissolve the formed crystals, solvent-mediated transformations lead to the more energetically favourable phase.<sup>10</sup> Therefore, the control over the nucleation process and solvent-mediated transformations are necessary to determine the polymorphism.

In the present system, oligomeric species are defined as square building blocks for  $1_{sq}$  and triangular building blocks for  $1_{kgm}$ , as described in a previous study.<sup>8a</sup> To discuss the stability of each oligomer, the conformation of the paddle-wheel unit in both structures was carefully examined. As shown in Fig. 1(c), the coordination geometry around the zinc ions, *i.e.* the structure of the paddle-wheel

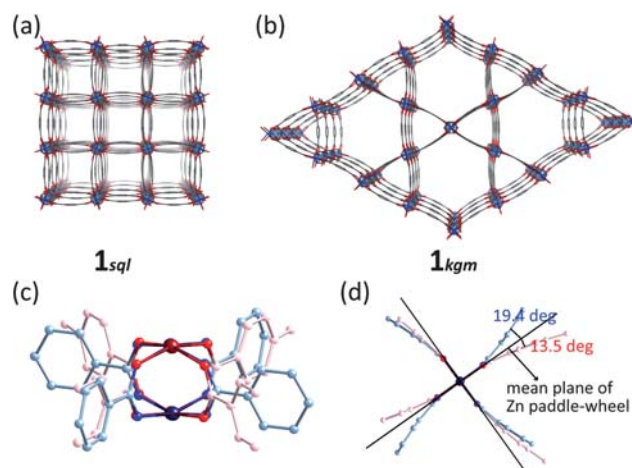


**Fig. 1** Crystal structures of (a)  $1_{sq}$  and (b)  $1_{kgm}$  along *c* axis, (c) conformations of a paddle-wheel unit in  $1_{sq}$  (blue line) and  $1_{kgm}$  (red line), and (d) the deviation of the bdc molecules from the mean plane of the paddle-wheel unit in  $1_{sq}$  (blue line) and  $1_{kgm}$  (red line). Hydrogen atoms and disordered guest molecules are omitted for clarity.

<sup>a</sup>Institute for Integrated Cell-Material Sciences (iCeMS), Kyoto University, Yoshida, Sakyo-ku, Kyoto 606-8501, Japan

<sup>b</sup>Department of Synthetic Chemistry & Biological Chemistry, Graduate School of Engineering, Kyoto University, Katsura, Nishikyo-ku, Kyoto 615-8510, Japan. E-mail: kitagawa@sbchem.kyoto-u.ac.jp

<sup>c</sup>ERATO Kitagawa Integrated Pores Project, Japan Science and Technology Agency (JST), Kyoto Research Park Bldg #3, Shimogyo-ku, Kyoto 600-8815, Japan. E-mail: shuhei.furukawa@kip.jst.go.jp

† Electronic supplementary information (ESI) available: A picture of  $1_{kgm}$ . Scheme S1, the result of peak fitting for **3**, PXRD patterns, and crystal structures of  $2_{kgm}$  and  $2_{sq}$ . CCDC reference number 769113. For ESI and crystallographic data in CIF or other electronic format see DOI: 10.1039/c004066e

unit in  $\mathbf{1}_{sql}$  and  $\mathbf{1}_{kgm}$  coincide. In contrast, the deviation of the bdc molecules from the mean plane of the paddle-wheel unit is significantly larger for  $\mathbf{1}_{sql}$  ( $19.41(7)^\circ$ ) compared to that of  $\mathbf{1}_{kgm}$  ( $13.5(1)^\circ$ , Fig. 1(d)). From this steric consideration, the triangular oligomer would be more stable than the square oligomer in solution, and thus the concentration of the triangular oligomer would be higher than that of the square oligomers. This hypothesis allowed us to design a synthetic experiment that traps the triangular species to form  $\mathbf{1}_{kgm}$  before the nucleation of  $\mathbf{1}_{sql}$  by just cooling the mixture at the beginning of the reaction. In contrast, in the crystalline state,  $\mathbf{1}_{sql}$  is thermodynamically favoured rather than  $\mathbf{1}_{kgm}$ ;  $\mathbf{1}_{sql}$  has a higher density as  $0.870 \text{ g cm}^{-3}$  than  $\mathbf{1}_{kgm}$  as  $0.730 \text{ g cm}^{-3}$ .<sup>8a</sup> Therefore,  $\mathbf{1}_{sql}$  is expected to be obtained from the reaction mixture when solvent-mediated transformations are allowed to proceed.

Based on the strategy described above, the syntheses of  $[\text{Zn}_2(\text{bdc})_2(\text{dabco})]_n$  polymorphs were performed. A mixture of  $\text{Zn}(\text{NO}_3)_2 \cdot 6\text{H}_2\text{O}$ ,  $\text{H}_2\text{bdc}$ , and dabco (2 : 2 : 1 in molar ratio) with the concentration of the Zn salt as 0.01 M was added to DMF (20 mL). After the suspension was sonicated for 30 min, the insoluble powder was filtered off and the resulting transparent solution was heated at  $120^\circ\text{C}$ . Note that this pre-treatment is the standard protocol to obtain a pure phase of  $\mathbf{1}_{sql}$  after a subsequent reaction time of 48 h. For  $\mathbf{1}_{kgm}$ , after heating for 0.5 h the solution was still transparent and the transparent solution was cooled down to  $25^\circ\text{C}$ . The hexagonal plate crystals were harvested (Fig. S1†). Both single crystal X-ray diffraction (SCXRD) and powder X-ray diffraction (PXRD) measurements determined the phase and purity of  $\mathbf{1}_{kgm}$  as expected (Fig. S2†).

To further document our protocol, reactions with various heating times (1, 1.5, 2, 12, or 48 h) followed by cooling were carried out (Scheme S1†). From 1.5 h of heating and onwards, crystals appeared before the cooling step (See also Table 1). The PXRD patterns of the crystals obtained after cooling to  $25^\circ\text{C}$  are summarized in Fig. 2. From Fig. 2, we can see that up to 1 h of pre-heating, only  $\mathbf{1}_{kgm}$  is obtained. Subsequent heating leads to the formation of an unknown intermediate (**3**), to finally form only  $\mathbf{1}_{sql}$  after 48 h. SCXRD measurements on **3** were performed, but the structural analysis was unsuccessful because of its low crystallinity. However, the intermediate PXRD patterns were analyzed by peak fitting. (See Fig. S3†). This analysis shows that **3** is single phased and can not correspond to either  $\mathbf{1}_{kgm}$  or  $\mathbf{1}_{sql}$ . The formation of **3** obscures the understanding the mechanism of polymorphism between  $\mathbf{1}_{kgm}$  and  $\mathbf{1}_{sql}$ . Therefore, the similar experiments for 0.03 and 0.1 M of the Zn salts were carried out keeping the molar ratio of the starting materials to avoid the formation of **3**. Although an acceleration of the reaction was observed at the higher concentration (0.03 M) as shown in Fig. S4† and Table 1, the sequential crystallization from  $\mathbf{1}_{kgm}$  to  $\mathbf{1}_{sql}$  corresponded to the standard conditions (0.01 M). For a concentration of

**Table 1** Summary of the products obtained at different concentrations and preheating periods.

	0.5 h	1 h	1.5 h	2 h	12 h	48 h
0.01 M	$\mathbf{1}_{kgm}^a$	$\mathbf{1}_{kgm}^a$	$\mathbf{1}_{kgm}^a + \mathbf{3}^b$	$\mathbf{1}_{kgm}^a + \mathbf{3}^b$	$\mathbf{3}^b$	$\mathbf{1}_{sql}^b$
0.03 M	$\mathbf{1}_{kgm}^a$	$\mathbf{1}_{kgm}^a + \mathbf{3}^b$	$\mathbf{1}_{kgm}^a + \mathbf{3}^b$	$\mathbf{3}^b$	$\mathbf{1}_{sql}^b + \mathbf{3}^b$	—
0.1 M	$\mathbf{1}_{kgm}^a$	$\mathbf{1}_{kgm}^b + \mathbf{1}_{sql}^b$	$\mathbf{1}_{kgm}^b + \mathbf{1}_{sql}^b$	$\mathbf{1}_{kgm}^b + \mathbf{1}_{sql}^b$	$\mathbf{1}_{sql}^b$	—

<sup>a</sup> Crystals obtained after cooling <sup>b</sup> Crystals obtained soon after preheating

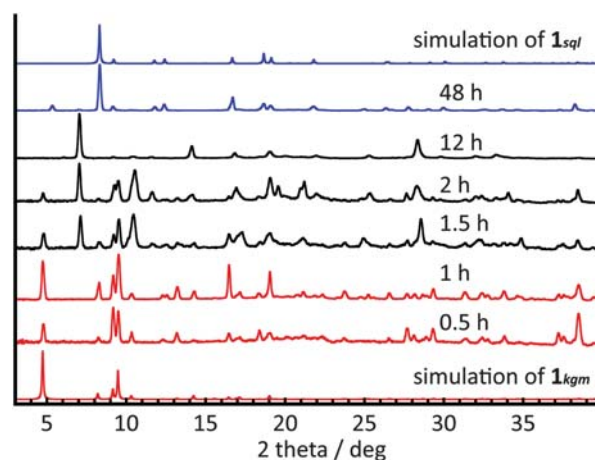


**Fig. 2** PXRD patterns of the products with various preheating times (0.5, 1, 1.5, 2, 12, and 48 h) after the cooling process and simulated patterns of  $\mathbf{1}_{kgm}$  and  $\mathbf{1}_{sql}$ . The concentration of zinc ions is 0.01 M.

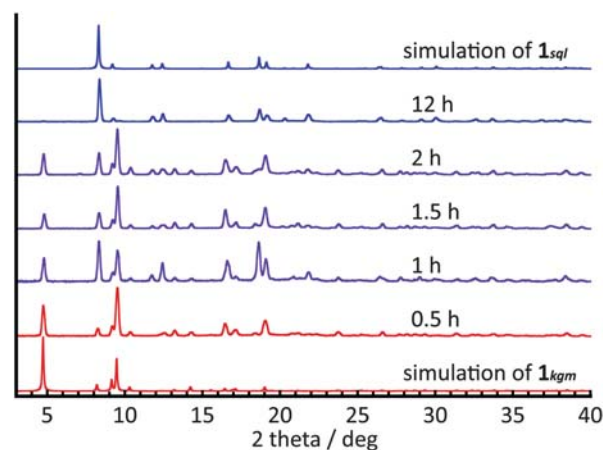


**Fig. 3** PXRD patterns of the products with various preheating times (0.5, 1, 1.5, 2, and 12 h) after the cooling process and simulated patterns of  $\mathbf{1}_{kgm}$  and  $\mathbf{1}_{sql}$ . The concentration of zinc ions is 0.1 M.

0.1 M, longer preheating times led to the precipitation of first  $\mathbf{1}_{kgm}$  and  $\mathbf{1}_{sql}$  to finally only crystallize  $\mathbf{1}_{sql}$ , already during the preheating time of 12 h (Fig. 3 and Fig. S5†) and the formation of **3** was avoided.

From these results, we can describe the plausible nucleation process of  $\mathbf{1}_{kgm}$  and  $\mathbf{1}_{sql}$  (concentration 0.1M) in terms of concentration of oligomers vs preheating time. Over the 1 h threshold, the precipitation of both  $\mathbf{1}_{kgm}$  and  $\mathbf{1}_{sql}$  occurs at  $120^\circ\text{C}$  because the concentration of the oligomers of  $\mathbf{1}_{kgm}$  and  $\mathbf{1}_{sql}$  is higher than the saturating concentration at  $120^\circ\text{C}$ . When the preheating time is extended, a solvent-mediated process prevails to result in  $\mathbf{1}_{sql}$  only if the reaction time is long enough to complete the transformation of all the products. In contrast, when the reaction mixture is heated for 0.5 h, both  $\mathbf{1}_{kgm}$  and  $\mathbf{1}_{sql}$  do not crystallize at  $120^\circ\text{C}$ ; the concentrations of both oligomers are too low to initiate the nucleation. When the still clear preheated reaction mixture is cooled to  $25^\circ\text{C}$ , however,  $\mathbf{1}_{kgm}$  can crystallize because the saturating concentration level for  $\mathbf{1}_{kgm}$  at  $25^\circ\text{C}$  is low enough to lead to the super-saturated state and the crystallization of  $\mathbf{1}_{kgm}$ . However,  $\mathbf{1}_{sql}$  cannot crystallize at  $25^\circ\text{C}$  because the saturating concentration is too high.

In summary on one hand, the pure phase of the pillared Kagomé layer framework of  $\mathbf{1}_{kgm}$  can be obtained by a short reaction time at 120 °C followed by the nucleation at 25 °C, thanks to the large difference of solubility of the oligomers at 120 °C and 25 °C. On the other hand, the pure phase of the pillared square-grid layer framework of  $\mathbf{1}_{sqf}$  can be obtained with a longer reaction time at 120 °C to initiate the nucleation and the solvent-mediated transformation process.

To validate our method, we extended this strategy to the synthesis of the new pillared Kagomé net framework using a longer pillar ligand, bpy,  $[\text{Zn}_2(\text{bdc})_2(\text{bpy})]_n$  ( $\mathbf{2}$ ). Therefore, a nucleation at a lower temperature was carried out; the mixture of  $\text{Zn}(\text{NO}_3)_2 \cdot 6\text{H}_2\text{O}$ ,  $\text{H}_2\text{bdc}$ , and bpy (2 : 2 : 1 in molar ratio) with the concentration of the Zn salt as 0.01 M was heated at 120 °C for 1 h, followed by cooling to 25 °C. After 1 day, the hexagon-shape crystals were harvested. The SCXRD measurement confirmed the formation of the novel framework with 2D Kagomé nets connected by bpy ligands ( $\mathbf{2}_{kgm}$ ) as shown in Fig. 4.

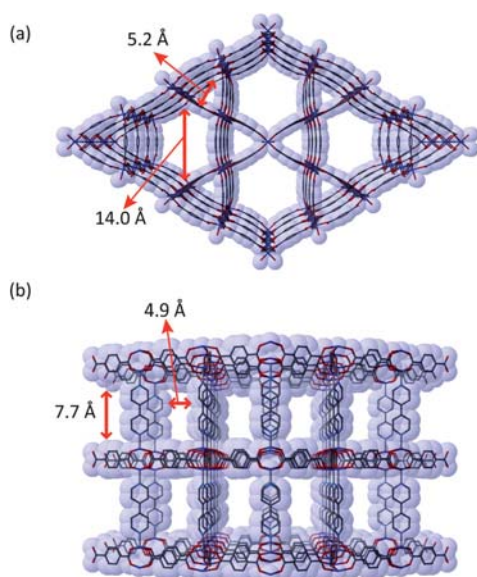


**Fig. 4** Crystal structures of  $\mathbf{2}_{kgm}$  along the  $c$  axis (a) the  $a$  axis (b). Disordered bpy molecules and hydrogen atoms are omitted for clarity.

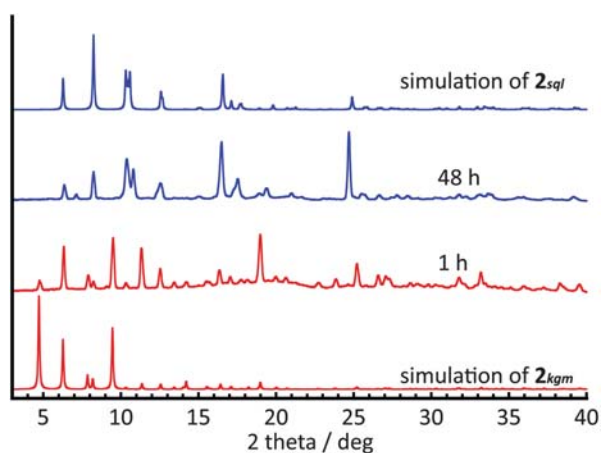


**Fig. 5** PXRD patterns of the products with various preheating times (1, and 48 h) after the cooling process and simulated patterns of  $\mathbf{2}_{kgm}$  and  $\mathbf{2}_{sqf}$ . The concentration of zinc ions is 0.01 M.

In this structure, the crystallographically imposed  $mmm$  and  $mm$  symmetries that are parallel to the  $\{110\}$  and  $\{100\}$  planes, respectively, generate Kagomé sheets and  $m$  symmetry that is parallel to the  $\{001\}$  plane, links the sheets by the pillar ligands. Whereas the framework of  $\mathbf{2}_{kgm}$  has the same 2D motif of Kagomé sheets as  $\mathbf{1}_{kgm}$ , the longer pillar linker as bpy connected the 2D Kagomé net in  $\mathbf{2}_{kgm}$  instead of dabco in  $\mathbf{1}_{kgm}$ . Thanks to the elongation of the pillar, the framework of  $\mathbf{2}_{kgm}$  has a larger pore window (7.7 Å × 4.9 Å) along the  $a$  axis rather than that of  $\mathbf{1}_{kgm}$  (3.5 Å × 4.9 Å). Similar to the reaction system of  $\mathbf{1}$ , the framework with 2D square-grid nets ( $\mathbf{2}_{sqf}$ )<sup>11</sup> was obtained after heating the reaction mixture for 48 h, but with a 2-fold interpenetration (Fig. 5 and Fig S6†). Even though the simple elongation of organic linkers normally results in the formation of the interpenetrated framework as seen in  $\mathbf{2}_{sqf}$ , the 2D Kagomé topology, however, allows for the modulation of the distance between Kagomé layers without reducing the void space by interpenetration; pillared Kagomé layers do not allow interpenetration due to the steric hindrance.

In conclusion, we succeeded in controlling the polymorphism in PCPs consisting of Zn ions, bdc, and dabco (for  $\mathbf{1}$ ) or bpy (for  $\mathbf{2}$ ) by solely adjusting the nucleation process systematically: a PCP with square grid net ( $\mathbf{1}_{sqf}$  and  $\mathbf{2}_{sqf}$ ) was obtained by using nucleation at high temperature (120 °C), whereas a PCP with Kagomé layers ( $\mathbf{1}_{kgm}$  and  $\mathbf{2}_{kgm}$ ) was obtained by a nucleation at room temperature (25 °C). The protocol described should open a new way to tune the connectivity between metal clusters by controlling the nucleation process. Moreover, we showed that the pillared 2D Kagomé nets are a suitable design to push the metrics and obtain larger pores without being confronted with the problems of interpenetration.

## Acknowledgements

M. K. is grateful to JSPS Research Fellowships for Young Scientists. We acknowledge Dr C. Bonneau, Dr A. Umemura and Dr N. Louvain for fruitful discussions.

## Notes and references

‡ The maximum symmetry representations, *i.e.* topological types, for  $\mathbf{n}_{sqf}$  and  $\mathbf{n}_{kgm}$  three-dimensional structures ( $n = 1, 2$ ) are **pcu** and **kag** respectively following the *Reticular Chemistry Structure Resource* nomenclature.<sup>13</sup>

§ **General Method:** Solvents and reagents were used as received from commercial sources unless noted otherwise.

**Measurement apparatus:** Single crystal X-ray diffraction measurements of  $\mathbf{1}_{kgm}$  and  $\mathbf{2}_{kgm}$  were performed with a Rigaku AFC10 diffractometer with Rigaku Saturn CCD system confocal monochromated Mo-K $\alpha$  radiation and data was processed using Crystal Clear-SM 1.4.0 (Rigaku). The structure was solved by direct methods and refined by full-matrix least-squares techniques on  $F^2$  (SHELXL-97).<sup>12</sup> All non-hydrogen atoms were anisotropically refined, while all hydrogen atoms were placed geometrically and refined with a riding model with  $U_{\text{iso}}$  constrained to be 1.2 times  $U_{\text{eq}}$  of the carrier atom. The diffused electron densities resulting from residual solvent molecules were removed from the data set using the SQUEEZE routine of PLATON and refined further using the data generated. The contents of the solvent region were estimated as one water molecule per asymmetric unit from the result of the SQUEEZE routine and included in the unit cell contents in the crystal data. Powder X-ray diffraction measurements were performed with Bruker D8 Discoverer with GADDS equipped with a sealed tube X-ray generator producing Cu-K $\alpha$  radiation.

**Crystal data for  $\mathbf{2}_{kgm}$ :**  $\text{C}_{26}\text{H}_{20}\text{N}_2\text{O}_{10}\text{Zn}_2$   $M_r = 651.18$ , hexagonal, space group  $P6/mmm$ , (#191),  $a = 21.619(8)$ ,  $c = 14.105(4)$  Å,  $V = 5709(4)$  Å<sup>3</sup>,  $Z = 3$ ,  $T = 223(2)$  K,  $\rho_c = 0.568$  g cm<sup>-3</sup>,  $\mu(\text{Mo-K}\alpha) = 0.651$  cm<sup>-1</sup>,  $2\theta_{\text{max}} = 55.0^\circ$ ,  $\lambda(\text{Mo-K}\alpha) = 0.71075$  Å, 45244 reflections measured, 2544 unique

( $R_{\text{int}} = 0.0578$ ), 2320 ( $I > 2\sigma(I)$ ) were used to refine 55 parameters, 1 restraints,  $wR^2 = 0.2446$  ( $I > 2\sigma(I)$ ),  $R_1 = 0.0852$  ( $I > 2\sigma(I)$ ),  $GOF = 1.148$ . **General synthetic protocols:** A mixture of  $\text{Zn}(\text{NO}_3)_2 \cdot 6\text{H}_2\text{O}$ ,  $\text{H}_2\text{bdc}$ , and dabco (2 : 2 : 1 in molar ratio) was added to DMF (20 mL) and sonicated for 30 min. The suspension was filtered off and transferred to a glass tube. The solution was heated at 120 °C in an oil bath for 0.5–48 h and the reaction mixture was kept in incubator (25 °C) for 24 h. **Synthesis of  $2_{\text{kgm}}$ :** A mixture of  $\text{Zn}(\text{NO}_3)_2 \cdot 6\text{H}_2\text{O}$  (59.6 mg, 0.2 mmol),  $\text{H}_2\text{bdc}$  (33.2 mg, 0.2 mmol), and 4,4'-bipyridine (15.6 mg, 0.1 mmol) was added to DMF (20 mL) and sonicated for 30 min. The obtained transparent solution was heated at 120 °C in oil bath for 1 h and the reaction mixture was kept in incubator (25 °C). Colourless hexagonal crystals of  $2_{\text{kgm}}$  were obtained after 24 h.

- (a) O. M. Yaghi, M. O'Keeffe, N. W. Ockwig, H. K. Chae, M. Eddaoudi and J. Kim, *Nature*, 2003, **423**, 705–714; (b) S. Kitagawa, R. Kitaura and S. Noro, *Angew. Chem., Int. Ed.*, 2004, **43**, 2334–2337; (c) G. Férey, C. Mellot-Draznieks, C. Serre and F. Millange, *Acc. Chem. Res.*, 2005, **38**, 217–225; (d) Z. Wang and S. M. Cohen, *Chem. Soc. Rev.*, 2009, **38**, 1315–1329; (e) Dincá and J. R. Long, *Angew. Chem., Int. Ed.*, 2008, **47**, 6766–6779; (f) R. E. Morris and P. S. Wheatley, *Angew. Chem., Int. Ed.*, 2008, **47**, 4966–4981; (g) D. Zacher, O. Shekhah, C. Wöll and R. A. Fischer, *Chem. Soc. Rev.*, 2009, **38**, 1418–1429.
- (a) R. Matsuda, R. Kitaura, S. Kitagawa, Y. Kubota, R. V. Belosludov, T. C. Kobayashi, H. Sakamoto, T. Chiba, M. Takata, Y. Kawazoe and Y. Mita, *Nature*, 2005, **436**, 238–241; (b) J. R. Li, R. J. Kuppler and H.-C. Zhou, *Chem. Soc. Rev.*, 2009, **38**, 1477–1504.
- (a) M. Fujita, Y. J. Kwon, S. Washizu and K. Ogura, *J. Am. Chem. Soc.*, 1994, **116**, 1151–1152; (b) J. Y. Lee, O. K. Farha, J. Roberts, K. A. Scheidt, S. T. Nguyen and J. T. Hupp, *Chem. Soc. Rev.*, 2009, **38**, 1450–1459.
- M. D. Allendorf, C. A. Bauer, R. K. Bhaktaa and R. J. T. Houka, *Chem. Soc. Rev.*, 2009, **38**, 1330–1352.

- (a) B. Rather, B. Moulton, R. D. B. Walsh and M. J. Zaworotko, *Chem. Commun.*, 2002, 694–695; (b) E. Tynan, P. Jensen, P. E. Kruger and A. C. Lees, *Chem. Commun.*, 2004, 776–777; (c) C.-C. Wang, W.-Z. Lin, W.-T. Huang, M.-J. Ko, G.-H. Lee, M.-L. Ho, C.-W. Lin, C.-W. Shih and P.-T. Chou, *Chem. Commun.*, 2008, 1299–1301; (d) A. X. Zhu, J.-B. Lin, J.-P. Zhang and X.-M. Chen, *Inorg. Chem.*, 2009, **48**, 3882–3889.
- (a) J. D. Dunitz and J. Bernstein, *Acc. Chem. Res.*, 1995, **28**, 193–200; (b) J. Bernstein, R. J. Davey and J.-O. Henck, *Angew. Chem., Int. Ed.*, 1999, **38**, 3440–3461; (c) N. R-Hornedo and D. Murphy, *J. Pharm. Sci.*, 1999, **88**, 651–660.
- D. N. Dybtsev, H. Chun and K. Kim, *Angew. Chem., Int. Ed.*, 2004, **43**, 5033–5036.
- (a) H. Chun and J. Moon, *Inorg. Chem.*, 2007, **46**, 4371–4373; (b) T. Friščić, D. G. Reid, I. Halasz, R. S. Stein, R. E. Dinnebieer and M. J. Duer, *Angew. Chem., Int. Ed.*, 2010, **49**, 712–715.
- (a) H. N. Miras, E. F. Wilson and L. Cronin, *Chem. Commun.*, 2009, 1297–1311; (b) D.-L. Long, C. Streb, Y. F. Song, S. Mitchell and L. Cronin, *J. Am. Chem. Soc.*, 2008, **130**, 1830–1832; (c) E. F. Wilson, H. Abbas, B. J. Duncombe, C. Streb, D.-L. Long and L. Cronin, *J. Am. Chem. Soc.*, 2008, **130**, 13876–13884; (d) H. N. Miras, G. J. T. Cooper, D.-L. Long, H. Bögge, A. Müller, C. Streb and L. Cronin, *Science*, 2010, **327**, 72–74.
- (a) P. T. Cardew and R. J. Davey, *Proc. R. Soc. Lond.*, 1985, **A 398**, 415–428; (b) R. J. Davey, N. Blagden, G. D. Potts and R. Docherty, *J. Am. Chem. Soc.*, 1997, **119**, 1767–1772.
- (a) B.-Q. Ma, K. L. Mulfort and J. T. Hupp, *Inorg. Chem.*, 2005, **44**, 4912–4914; (b) B. Chen, C. Liang, J. Yang, D. S. Contreras, Y. L. Clancy, E. B. Lobkovsky, O. M. Yaghi and S. Dai, *Angew. Chem., Int. Ed.*, 2006, **45**, 1390–1393.
- G. M. Sheldrick, *Program for Crystal Structure Refinement*, University of Göttingen, Germany, 1997.
- M. O'Keeffe, M. A. Peskov, S. Ramsden and O. M. Yaghi, *Acc. Chem. Res.*, 2008, **41**, 1782.